

## Regeneration of diabetic axons is enhanced by selective PTEN knockdown

Journal:	<i>Brain</i>
Manuscript ID:	Draft
Manuscript Type:	Original Article
Date Submitted by the Author:	n/a
Complete List of Authors:	<p>Singh, Bhagat; University of Calgary, Clinical Neurosciences and Hotchkiss Brain Institute</p> <p>Singh, Vandana; University of Calgary, Clinical Neurosciences and Hotchkiss Brain Institute</p> <p>Krishnan, Anand; University of Calgary, Clinical Neurosciences and Hotchkiss Brain Institute</p> <p>Koshy, Kurien; University of Calgary, Clinical Neurosciences and Hotchkiss Brain Institute</p> <p>Martinez, Jose; University of Calgary, Clinical Neurosciences and Hotchkiss Brain Institute</p> <p>Cheng, Chu; University of Calgary, Clinical Neurosciences and Hotchkiss Brain Institute</p> <p>Almquist, Chris; University of Calgary, Clinical Neurosciences and Hotchkiss Brain Institute</p> <p>Zochodne, Douglas; University of Calgary, Department of Clinical Neurosciences, Room 168</p>
Key Words:	
Please choose up to 5 keywords from the list:	diabetic polyneuropathy, Diabetes, peripheral nervous system, Peripheral nerve, axonal injury

## Regeneration of diabetic axons is enhanced by selective PTEN knockdown

**B. Singh**<sup>1</sup>, V Singh<sup>1\*</sup>, A Krishnan<sup>1\*</sup>, K Koshy<sup>1</sup>, Jose A. Martinez<sup>1</sup>, Chu Cheng<sup>1</sup>, Chris Almquist<sup>1</sup>, DW Zochodne<sup>1\*\*</sup>

<sup>1</sup>Department of Clinical Neurosciences and the Hotchkiss Brain Institute, University of Calgary, Calgary, AB, Canada

\*Contributed equally to the work

\*\*Corresponding Author:

Douglas W Zochodne, 168 Heritage Medical Research Bldg; 3330 Hospital Dr. NW, Department of Clinical Neurosciences and the Hotchkiss Brain Institute, University of Calgary, Calgary, Alberta, Canada T2N 4N1.

Email: dzochodn@ucalgary.ca

Contact Number: Office: (403) 220-8759, Lab: (403) 220-8539, Fax: (403) 283-8731

**Abstract:**

Diabetes mellitus renders both widespread and localized, but irreversible damage to peripheral axons while imposing critical limitations on their ability to regenerate. A major failure of regenerative capacity thereby imposes a 'double hit' in diabetic patients. The mechanisms of diabetic neuron regenerative failure have been speculative and few approaches have offered therapeutic opportunities. In this work we identify an unexpected but major role for PTEN (phosphatase and tensin homolog deleted on chromosome ten) upregulation in diabetic peripheral neurons in attenuating axon regrowth. In two chronic diabetic neuropathy models in mice, we identified significant PTEN upregulation in peripheral sensory neurons at the mRNA and protein level, compared to littermate controls. *In vitro*, sensory neurons from these mice were capable of responding to PTEN knockdown with substantial rises in neurite outgrowth and branching. To test regenerative plasticity in a chronic diabetic model with established neuropathy, we superimposed an additional focal sciatic nerve crush injury and assessed morphological, electrophysiological and behavioural recovery. Retrograde knockdown of PTEN in dorsal root ganglia (DRG) ipsilateral to the side of injury was achieved using a unique form of nonviral siRNA delivery to the nerve injury site. In comparison to scrambled sequence control siRNA, PTEN siRNA improved several facets of regeneration: recovery of compound muscle action potentials, reflecting numbers of reconnected motor axons to endplates, conduction velocities of both motor and sensory axons, reflecting their maturation during regrowth, numbers and caliber of regenerating

myelinated axons distal to the injury site and reinnervation of the skin by unmyelinated epidermal axons. Collectively, these findings identify a novel therapeutic approach and target, PTEN, for diabetic neuroregenerative failure.

For Peer Review

Diabetes mellitus (DM), a health burden of enormous and growing prevalence, is the most common cause of damage to the peripheral nervous system. Diabetes renders diffuse nerve damage, or polyneuropathy, as well as focal damage known as mononeuropathy [Dyck *et al.* 1993;Zochodne 1999]. Polyneuropathy is a progressive neurodegenerative disorder that particularly targets sensory neurons and their axons, starting in their distal terminals [Zochodne *et al.* 2008]. In addition to polyneuropathy and mononeuropathy, however, diabetes substantially attenuates axon regeneration and recovery, imposing a 'double hit' on the nervous system [Ishii and Lupien 1995;Kennedy and Zochodne 2000;Kennedy and Zochodne 2005b;Longo *et al.* 1986;Terada *et al.* 1998]. While several mechanisms of neuroregenerative failure in diabetes have been considered, few have offered robust avenues for repair [Ishii and Lupien1995;Kennedy and Zochodne 2002;Terada, Yasuda, and Kikkawa1998;Triban *et al.* 1989;Xu *et al.* 2002;Xu and Sima 2001;Yasuda *et al.* 1999;Yasuda *et al.* 2003].

Diminished intrinsic regenerative capacity of mature neurons is a major aspect of regeneration failure. Given this limitation, removal of extracellular inhibitory cues and addition of growth factors may not be not sufficient to accomplish the desired regeneration outcomes [Brewster *et al.* 1994;GrandPre *et al.* 2002;Mukhopadhyay *et al.* 1994;Schnell *et al.* 1994]. Most growth factors offer selective support for only the neuron subclasses that express appropriate receptors. In diabetes, growth factor receptors are downregulated [Zochodne *et al.* 2001] and neuropathic damage involves a wide spectrum of axons, especially sensory [Malik *et al.* 2001]. PTEN is a key and widely expressed intrinsic neuronal mechanism that regulates axonal regrowth through inhibition of PI3K-pAkt, a central pathway involved in survival, growth, proliferation, and

regeneration of axons [Gallo and Letourneau 1998; Jones *et al.* 2003; Soltoff *et al.* 1992]. PI3K activation through growth factor tyrosine kinase receptors generates phosphatidylinositol 3,4,5 triphosphate (PIP3) which in turn translocates the serine/threonine kinase Akt to plasma membranes. There it is phosphorylated and thereby activated through phosphoinositide-dependent kinase (PDK-1) [Carter and Downes 1992] [Raffioni and Bradshaw 1992]. Specifically PTEN inhibits PI3K-pAkt signaling by dephosphorylating PIP3 [Leslie and Downes 2002]. One key downstream consequence of attenuated pAkt signaling is increased levels of GSK-3 $\beta$ , a molecule that promotes growth cone collapse [Eickholt *et al.* 2002; Park *et al.* 2010]. Deletion of PTEN enhanced regeneration of corticospinal tract and retinal ganglionic cells (RGCs) in the CNS [Liu *et al.* 2010; Park *et al.* 2008] and axons of peripheral sensory neurons [Christie *et al.* 2010]. After axon injury, PTEN expression in peripheral neurons persists, erecting an ongoing regenerative roadblock despite the need for plasticity in regrowing neurons. However dismantling the roadblock by PTEN inhibition or siRNA knockdown substantially increases neurite outgrowth from adult sensory neurons *in vitro* and accelerates the outgrowth of peripheral axons beyond a nerve transection. Since PTEN attenuates common transduction pathways activated by a number of growth factors, its inhibition or knockdown encourages a wide spectrum of neurons to grow.

In this work, we explored whether augmenting intrinsic neuron growth through PTEN knockdown in diabetic neurons might allow them to overcome their inherent growth limitations. Unexpectedly, we found that expression of the PTEN roadblock was elevated in diabetes. Adult diabetic sensory neurons had robust responsiveness to its knockdown *in vitro* whereas *in vivo* its knockdown accelerated recovery of several

facets of nerve regrowth in a chronic model of diabetic polyneuropathy. PTEN knockdown was accomplished by a unique and selective form of delivery to injured neurons through retrograde uptake of an siRNA.

## Materials and Methods

**Induction of diabetes, injury:** Outbred adult 18-20g CD-1 mice (Charles River, Canada), and db/db (BKS.Cg-Dock7m +/- Leprdb/J) mice (Jackson Labs) were used in the study. The procedures were reviewed and approved by the University of Calgary Animal Care Committee in conjunction with guidelines from the Canadian Council of Animal Care (CCAC). Mice were made diabetic by 3-day consecutive injections of intraperitoneal (i.p.) streptozotocin (STZ, Sigma) at a dose of 85, 70 and 55 mg/kg dissolved in citrate buffer (pH 4.5). Control animals received i.p. citrate buffer alone. Diabetes status was confirmed as  $\geq 16$  mmol/l fasting using a Glucometer (Ultra one). Under isoflurane anaesthesia, and using aseptic techniques the left sciatic nerve of diabetic mice (n=7-8/group) was exposed and crushed just distal to the sciatic notch with a sterile forceps for 15 seconds.

**PTEN expression:** For immunohistochemistry, published methods were followed [Kan *et al.* 2012]. In brief, DRGs were harvested and fixed in modified Zamboni's fixative (2% PFA, 0.5% picric acid and 0.1% PBS) overnight at 4<sup>0</sup>C and then cryoprotected in 20% sucrose/PBS. After embedding in optimum cutting temperature (OCT) compound (Miles), 14 $\mu$ m thick sections were placed onto poly-L-lysine coated glass slides. Primary antibodies applied were monoclonal anti-NF200 (heavy subunit of neurofilament, axons,

1:800, Sigma) and rabbit polyclonal PTEN (1:50; Santa Cruz) and incubated at 4<sup>0</sup>C for 24h. The following day, slides were washed with PBS and incubated with secondary antibodies, anti-mouse IgG CY3 conjugate (1:100, Sigma) or Alexa Fluor 488 goat anti-rabbit IgG (H + L) conjugate (1:400, Cedarlane) for 1h at room temperature (RT). Finally, cover slips were mounted on the slides with bicarbonate buffered glycerol (pH 8.6) and the slides were viewed with a fluorescent microscope (Zeiss Axioskope). Negative controls included omission of primary antibodies on parallel sections (not shown). Pixel intensity measurements and analysis was performed using Adobe Photoshop CS4 (Adobe Systems). For semiquantitative analysis of PTEN expression in neurons, they were divided into four categories of arbitrary intensity levels: > 100 (arbitrary units) were considered positive, medium (100–150), strong (150-200) and very strong (> 200). Measurements included the total number of neurons in each category. A total of 3 sections per mouse were analysed (approximate 250–500 neurons/mouse). For neuronal size analysis, luminosity and size of each neuron from n=3 DRG sections/group (approximately 400-500 neurons from each of control and diabetic group) were measured provided they were approximately centrally sectioned, as indicated by DAPI nuclear staining. Luminosity and size was measured using Image J (NIH software). Neuronal size and their respective luminosities were plotted on a graph by subdividing neurons into a pool of >15 μm, 15-20 μm, 20-30 μm, 30-40 μm and >40 μm based on their size. To confirm the retrograde transport of PTEN siRNA, we ligated the sciatic nerve proximal to the injury site. Fluorescent-labeled PTEN siRNA (Cat. # SI02734494, Mm\_PTEN\_6) was applied for 6 days, at the injury site with additional intraplantar injections each day. On day 7, mice were perfused and tissue

samples were processed as above. Fourteen micron thick longitudinal sections of sciatic nerves and 10µm thick transverse sections of DRGs were dried, washed with PBS buffer for three times. Sciatic samples were mounted and covers slipped and were visualized with an Olympus laser scanning confocal microscope equipped with epifluorescence (60× magnification and scanning step size 1 µm). The DRG sections were immunostained with PTEN and visualized with Zeiss Axioskope fluorescent microscope.

**Analysis of regenerating axons:** Ipsilateral, tibial nerves distal (~10mm) to the crush site and footpads were harvested at 21 day after sciatic injury. Tibial nerves were fixed in glutaraldehyde (2.5%) buffered in cacodylate (0.025 M) overnight, washed and stored in cacodylate buffer (0.15 M), then fixed in osmium tetroxide (2%), washed in graded alcohols then embedded in epon [Ohnishi *et al.* 1976]. Transverse sections of 1µm thickness were made through the approximate centre of the tibial nerve and stained with toluidine blue. The whole nerve sections were photographed under oil immersion microscopy (100X) in non-overlapping fields. In each field, the numbers and caliber of unequivocal myelinated axons were then measured using an image analysis program (Scion image) by an observer blinded to treatment groups. Final measurements included total number and mean axonal diameter of regenerating myelinated axons. Footpad skin samples were harvested using skin punch and processed as described previously [Kan, Guo, Singh, Singh, and Zochodne 2012]. Briefly, samples were fixed in 2% PLP [PFA (2%), L-lysine and sodium periodate) for 18h at 4°C and cryoprotected overnight in 20% glycerol/0.1 M Sorrenson phosphate buffer at 4°C. Skin sections of 25µm thickness were blocked in 10% goat serum for 1h at RT. Primary antibody

PGP9.5 (rabbit polyclonal; 1:1000, Encore biotechnology) was applied overnight at 4°C followed by goat anti-rabbit Cy3; 1:100 (Jackson immunoresearch) secondary for 1h at RT. Images were captured using an Olympus laser scanning confocal microscope (100× magnification and step size of 1 μm). Epidermal fibers labeled with PGP9.5 were counted in five adjacent fields of six sections for a total 30 fields per mouse at each time point. Both vertical (trajectory approximately 90° to the surface of the skin) and total (all axon profiles) were analyzed. All analyses were conducted with the examiner blinded to the identity of the samples being studied.

**Electrophysiology:** Multifiber motor and sensory conduction recordings were carried out in left sciatic–tibial fibers in mice anesthetized with isoflurane at near-nerve subcutaneous temperature of 37°C, maintained by a thermosensitive heat lamp as previously described [Kan, Guo, Singh, Singh, and Zochodne2012].

**Functional recovery of sensation:** Mice underwent mechanical (Von Frey filaments) and thermal testing (Hargreaves test) at day 0 (before crush injury), 14 and 28 days following sciatic nerve crush with and without PTEN siRNA, as described above. There were 5 min intervals provided between a total of three trials performed during the same day. To test mechanical sensitivity of the foot, withdrawal in response to a stimulus consisted of increasing amount of force using calibrated (4–26 g) Von Frey monofilaments (Stoelting, Wood Dale, IL) applied to the plantar surface of the paw to a mouse habituated within a plexiglass cage with holes in the flooring to allow application. Each paw was probed three times for ~1s to the plantar surface with enough force to

cause slight flexion of the monofilament. For testing the recovery of thermal sensation, we used the Hargreaves apparatus [Hargreaves *et al.* 1988]. In brief, a radiant heat source was applied individually to the middle of either hindpaw and the latency (seconds) to withdrawal was measured. Three separate trials were performed for the withdrawal response. Mechanical and thermal testing was performed on identical days with an interval of at least 1h between the two tests.

**Western immunoblots:** DRGs (L4-L6) and sciatic nerve samples were added to RIPA lysis buffer (Fisher Scientific) containing protease and phosphatase inhibitors (Roche). As previously described [Singh *et al.* 2012], 20 $\mu$ g of total protein was electrophoresed on 10% SDS-PAGE and then transferred on PVDF membrane in Tris-glycine-methanol buffer for 2h at 4°C. After blocking with 5% nonfat dry milk, membranes were incubated overnight with a polyclonal antibody to PTEN, 1:1000 (Mouse monoclonal; Cell Signaling), ps6k, 1:1000 (rabbit polyclonal; Cell Signaling), and tubulin or actin, 1:1000 (mouse monoclonal; Santa Cruz) as a loading control in 2% BSA in TBS (Tris buffer saline). The next day, after TBST [TBS with Tween 20 (0.1%)] rinses, horseradish peroxidase-labeled (HRP) secondary antibodies, anti-rabbit IgG HRP and anti-mouse IgG HRP (Santa Cruz), were incubated with the immunoblot at 1:5000 dilutions for 1h at RT. The signals were developed by exposing the blot to enhanced chemiluminescent reagents (Amersham) and subsequently exposure on Hyperfilm (GE Healthcare). The film images were digitized and the difference between the treatments was measured by analyzing pixel intensity and the size of the band using Photoshop (Adobe).

**qRT-PCR:** qRT-PCR was performed according to previous descriptions [Christie, Webber, Martinez, Singh, and Zochodne 2010]. Briefly, total RNA was extracted using

Trizol reagent (Invitrogen) and first strand DNA was synthesized utilizing SuperScript II First-strand Kit (Invitrogen). Real time quantitative PCR was performed on the Step One Plus sequence detection system (Applied Biosystems). Primers of interest were designed with Primer Express 2.0 (Applied Biosystems) and synthesized by the University of Calgary DNA Lab. The purity of each amplicon was determined using melting curve analysis. Quantification of amplified products was done using the SybrGreen I fluorophore (Invitrogen). The cycle number at which the fluorescence signal crossed a fixed threshold (threshold cycle, CT) with an exponential growth of PCR product during the linear phase was recorded. Relative expression values were generated using the comparative CT method ( $2^{-\Delta\Delta CT}$ ) where all genes of interest were standardized to expression of RPLP0. Primer sequences were as follows: PTEN:F,5'-GATAGCCCTAACCCCAAGAACG-3';R,5'-TGAAACCTCCCATGTGCTGAT-3' ;RPLP0: F, 5'-AAGAACACCATGATGCGCAAG-3'; R, 5'-TTGGTGAACACGAAGCCCA-3'

***In vitro* studies of adult sensory neurons:** The procedure for adult sensory neuronal cell culture was similar to previous work [Andersen *et al.* 2000;Lindsay 1988;Singh, Xu, McLaughlin, Singh, Martinez, Krishnan, and Zochodne2012;Webber *et al.* 2011b]. L4-L6 DRGs were dissected from adult wild type and diabetic mice washed with Hank's balanced salt solution (HBSS) and dissociated by incubating in L15 medium containing 0.1% collagenase (90 min, 37<sup>0</sup>C) followed by trituration and then passage through a 70 $\mu$ m mesh. To partially remove SCs, the cell suspension was loaded onto 15% BSA (Sigma) in L15 and spun at 1000 rpm for 5 min. One ml of growth medium [DMEM/F12 (Invitrogen) containing N2 nutrients supplement (Invitrogen), 10 $\mu$ M cytosine  $\beta$ -D-

arabinofuranoside hydrochloride (Sigma), 5U ml<sup>-1</sup> penicillin-streptomycin (Invitrogen)] was added to each dish. Scrambled and fluorescent PTEN siRNA was prepared in BSA free media with 1:10 ratio of transfection buffer (Invitrogen) and was applied at a 20nM dose. Sensory neurons were viewed by phase contrast using an inverted microscope (Zeiss Axiovert 40 CFL). Forty-eight hours later, neurons were fixed with 2% PFA for 2h at 4°C followed by PBS and then blocked with 10% goat serum (0.3% tritonX100/PBS1x) for 30 minutes at RT. Neurons and neurites were stained with 1h incubation of mouse monoclonal Nf-200 antibody (1:800, Sigma) at room temperature (RT). Secondary antibody, sheep anti-mouse IgG (whole molecule), F(ab)<sub>2</sub> fragment-Cy3 (1:200; Sigma) was applied following PBS wash at RT for 1h. The samples were then washed in PBS and mounted using DAPI vectashield (Vector laboratories) to label the nuclei and imaged using a Zeiss Axioscope fluorescent microscope. The total neurite outgrowth, number of primary neurites (defined as processes extending from the soma), length of the longest neurite and number of branches of a primary neurite were analyzed and quantified by MetaXpress software and an observer blinded to the treatment condition (Molecular Devices).

**Statistical analysis:** Results were represented as mean  $\pm$  SEM and compared with a one way ANOVA with post hoc Tukey's comparisons, or student's t-tests (one tailed in an expected direction of change) as appropriate.

## Results

### (i) PTEN expression is elevated in diabetic peripheral sensory neurons

Previous work has suggested that neurons with elevated expression of PTEN, particularly the small caliber IB4 population, have attenuated intrinsic growth characteristics [Christie, Webber, Martinez, Singh, and Zochodne2010;Leclere *et al.* 2007]. We examined mRNA and protein expression of PTEN in experimental diabetes, known to exhibit marked evidence of regenerative failure [Kennedy and Zochodne2000]. Diabetic DRGs (dorsal root ganglia) had elevated levels of PTEN compared to littermate controls, verified using several approaches. Firstly, we identified rises in PTEN mRNA in DRGs of a mouse model of type 1 DM induced by streptozotocin (STZ), with a duration of diabetes of 3 months (**Figure 1a**). Next we confirmed elevated expression of PTEN protein levels, by Western immunoblots in both diabetic DRGs and sciatic nerves (**Figure 1b,c [day 0, basal] and supplementary figure 1**). To confirm that upregulated PTEN in DRGs specifically involved neurons, we examined two separate diabetes models, STZ-induced diabetes of 3 months in outbred CD-1 mice, a model of type 1 diabetes and db/db mice at 12 weeks of age, a model of type 2 DM (**Figure 1d**). We noted prominent neuronal expression, particularly involving small caliber sensory neurons, as previous reported [Christie, Webber, Martinez, Singh, and Zochodne2010]. Using a neuronal size expression analysis however, we noted that in diabetes, PTEN expression was also upregulated in medium to large caliber neurons, unlike controls (**Figure 1e**). Using a semi-quantitative luminosity analysis, under identical conditions of staining and imaging, we also confirmed that higher numbers overall, of sensory neurons, expressed PTEN (**Figure 1f**). PTEN is normally associated with downregulation of downstream pS6 ribosomal protein, a molecule essential for protein synthesis and growth cone formation [Park, Liu, Hu, Kanter, and He2010]. Although we

were unable to confirm overall changes in pAkt in diabetes (data not shown), levels of ps6k in diabetic DRGs were substantially lower than nondiabetic controls and its expression involved DRG sensory neurons (**Figure 1i,j**). Taken together, these findings identified a substantial upregulation of PTEN in larger numbers of expressing neurons and a shift in the populations that express it. Finally, we asked whether PTEN upregulation in diabetes persists following injury, where it may dampen regenerative activity. In previous work, while PTEN levels have declined following injury, persistent expression continues to inhibit axon regrowth [Christie, Webber, Martinez, Singh, and Zochodne2010]. Thus while PTEN declined following injury, its mRNA and protein expression in diabetic DRGs were nonetheless higher than in nondiabetic neurons (**Figure 1b,g, h**).

#### (ii) Diabetic neurons are responsive to PTEN inhibition

We next tested whether adult diabetic sensory neurons retained their ability to respond to PTEN inhibition *in vitro*. Previously, we showed that nondiabetic neurons increased neurite outgrowth and branching in response to PTEN inhibition or knockdown, a rise in plasticity that translated into enhanced *in vivo* outgrowth [Christie, Webber, Martinez, Singh, and Zochodne2010]. At the 2 DIV (days *in vitro*) time point studied here baseline neurite outgrowth of adult diabetic DRG neurons was not impaired, a change identified in other models of longer duration (**Figure 2**) [Zherebitskaya *et al.* 2009]. Despite this caveat, fluorescent PTEN siRNA was incorporated in sensory neurons (**Figure 2a**), knocked down PTEN mRNA (**Figure 2b**) and generated a robust increase in neurite outgrowth and branching (**Figure 2c-g**).

### **(iii) Knockdown of PTEN by nonviral retrograde siRNA uptake**

To provide selective knock down of PTEN expression strictly in regenerating peripheral neurons, we exploited nonviral siRNA retrograde axon uptake from the injury site, an approach we have previously identified as capable of knocking down ipsilateral parent neuron gene expression [Webber *et al.* 2011a]. An important advantage of this approach, for potential translation into human work, is that viral vectors are not required for delivery. We applied Gelfoam soaked in PTEN or scrambled siRNA at a nerve crush injury site in nondiabetic control mice immediately for 20 min. then by percutaneous injection at the sciatic notch, supplemented with intraplantar injections daily for 5 days. PTEN mRNA and protein were reduced and ps6K protein appeared to be upregulated in ipsilateral DRGs at day 7 and PTEN protein decreased in the sciatic nerve (**Figure 3a-c and Supplementary figure 2**). By immunohistochemistry, there was a qualitative reduction in the intensity of PTEN expression in ipsilateral DRG neuronal cell bodies (**Figure 3d**). To provide evidence for retrograde transport of the siRNA, we ligated the sciatic nerves proximal to the injury, injected a 3'-alexa fluor 488 labeled siRNA into the crush zone and plantar footpads and noted accumulation of labelled nucleotide distal to the ligation site (**Figure 3e**). PTEN siRNA had no impact on blood glucose and body weights (data not shown).

### **(iv) PTEN inhibition accelerates electrophysiological recovery after injury in mice with chronic diabetes**

We next addressed whether PTEN inhibition might impact neuroregenerative failure in a chronic model of experimental diabetes. Neuropathy relevant models replicate several findings in humans that include electrophysiological abnormalities, axon atrophy, loss of sensation and retraction of epidermal axons. When a focal nerve injury, or mononeuropathy, is then superimposed, epidermal reinnervation, myelinated fiber regrowth and electrophysiological maturation are all significantly impaired in diabetes [Kennedy and Zochodne 2000; Sima *et al.* 1988]. Our 2 month diabetic mice developed expected and robust features of the model prior to injury: severe hyperglycemia, lesser weight gain (**Figure 4a,b**), slowing of motor and sensory conduction velocities (**Figure 4c,d**) and loss of thermal and mechanical sensitivity (**Figure 4g,h**). We then superimposed focal sciatic crush injury to address regeneration.

After crush injury, compound muscle action potentials (CMAPs) and sensory nerve action potentials (SNAPs) disappear, then gradually reappear at lower amplitudes as reconnection to targets is established (**Figure 5a,b,g,h**). Similarly, motor and sensory conduction velocities of regenerating axons at 14 and 28d post injury trended below pre-injury levels, consistent with their immaturity (**Figure 5c-f**) and at most time points were lower in diabetic mice. Ipsilateral PTEN retrograde siRNA knockdown enhanced repair of three of four electrophysiological indices of recovery in diabetic mice: CMAP amplitudes and conduction velocities of motor and sensory axons. In nondiabetic mice, the impact was less robust: a trend toward improved CMAPs and improved sensory conduction velocity. Interestingly, the magnitude of improvement in diabetics was large, rendering some values, such as motor conduction velocity, that exceeded control values (**Figure 5 c-f**).

**(v) PTEN inhibition accelerates myelinated axon regrowth and skin reinnervation**

We next examined whether PTEN retrograde siRNA knockdown influenced the repopulation of newly regenerated myelinated axons distal to the crush zone three weeks after injury. In keeping with previous observations of neuroregenerative failure, the numbers and mean caliber of myelinated axons in regenerating tibial nerves were substantially lower in diabetic mice (**Figure 6a-c**). In diabetic, but not nondiabetic nerves, ipsilateral to PTEN knockdown there was an increase in both the number and mean axon caliber of regenerating myelinating axons (**Figure 6a-c**).

Reinnervation of the skin target organ involves fine unmyelinated afferent fibers that repopulate the epidermis. Since PTEN expression was especially high in parent neurons of small caliber axons in the DRG, it was important to establish their responsiveness to knockdown. Similarly, loss of epidermal afferents is a key feature of diabetic neuropathies [Polydefkis *et al.* 2001]. The density of axons, IENFD (intraepidermal nerve fiber density) reinnervating the epidermis 3 weeks after sciatic nerve injury was substantially reduced compared to uninjured values (not shown), most marked in diabetics. As in previous work in our laboratory, we measured both vertically oriented axon profiles and total profiles so that all branching behaviour could be included [Cheng *et al.* 2010]. PTEN retrograde siRNA knockdown was associated with a significant increase in total and vertically directed epidermal axons in diabetic mice. In controls, there were only nonsignificant trends toward improvement (**Figure 6 d-f**). Behavioural sensory changes following sciatic nerve injury (**Supplementary Figure 3**)

proved a less robust marker of injury and recovery, likely because the sciatic nerve is not the sole contributor to hindpaw innervation. No significant changes in thermal sensitivity following injury were demonstrable beyond trends toward lesser sensitivity and there was no clear impact of PTEN knockdown. In both nondiabetics and diabetic mice there were nonsignificant trends toward heightened mechanical sensitivity after injury. In diabetic mice, PTEN knockdown was associated with greater mechanical sensitivity at 28d following injury.

## Discussion

The major findings of this work were (i) peripheral sensory neurons substantially upregulated PTEN expression at the mRNA and protein level during chronic diabetes; (ii) peripheral sensory neurons from diabetic mice were capable of responding to PTEN knockdown with evidence of increased plasticity; (iii) injured peripheral nerve axons took up local siRNA, delivered it by retrograde transport to their perikarya and knocked down PTEN mRNA; (iv) selective PTEN knockdown in injured diabetic neurons and axons accelerated regrowth: motor axon reconnection to endplates, electrophysiological maturation of motor and sensory axons, regrowth and maturation of myelinated axons and reinnervation of the epidermis. These benefits were more robust and consistent than those conferred by a similar strategy in injured nondiabetic nerves.

Several aspects of this project were specifically designed to mimic clinical scenarios. Over 50% of diabetic subjects have evidence of polyneuropathy [Dyck, Kratz, Karnes, Litchy, Klein, Pach, Wilson, O'Brien, Melton, and Service1993] identified by clinical loss

of sensation, loss of epidermal innervation of the skin and electrophysiological abnormalities, especially slowing of motor and sensory conduction velocity [Bril 1994]. We have previously provided evidence that the outbred diabetic mouse model, generated by STZ injection to model type 1 DM, as used in this work, provides robust modeling of these features [Kennedy and Zochodne 2005a]. Moreover, this diabetic model demonstrates severe regenerative failure when a focal injury is superimposed [Kennedy and Zochodne 2000]. In the present study, our mice had evidence of polyneuropathy after 2 months of diabetes with slowing of motor and sensory conduction velocity and loss of sensation to thermal and mechanical stimuli prior to injury.

Regeneration in diabetic peripheral nerves is a significant clinical consideration. For example, focal nerve injuries, mononeuropathies, are commonly identified in patients with pre-existing polyneuropathy. Examples include entrapment neuropathies at the carpal tunnel and cubital fossa or ischemic neuropathies. In addition, established neuropathy is difficult to reverse even in the setting of tight glycemic control or pancreatic transplantation [Kan, Guo, Singh, Singh, and Zochodne 2012; Kennedy *et al.* 1990; Mehra *et al.* 2007]. Targeted approaches to reverse abnormalities by exploiting axon regrowth is therefore a compelling therapeutic priority.

In this work, we addressed specific and clinically relevant regenerative endpoints. The CMAP amplitude correlates with the numbers of motor axons that regrow and reconnect to tibial motor endplates. Its recovery after crush injury is a functional measure of axon reconnection. Conduction velocities in regenerating motor and sensory axons are indices of maturation: regrowth of axon caliber, remyelination and re-insertion of nodal

and paranodal proteins. These electrophysiological endpoints were improved following PTEN knockdown. We examined numbers and caliber of myelinated axons distal to the crush zone and identified improvements in nerves following PTEN knockdown. Finally we identified enhanced reinnervation of the skin by fine unmyelinated axons. While we did demonstrate that mice with PTEN knockdown exhibited greater mechanical sensitivity at 28d, behavioural sensory data in mice after selective nerve injury can be difficult to interpret, a feature also observed in the present study. Since hindlimbs are also innervated by the saphenous nerve, mice (or rats) undergoing sciatic injury do not demonstrate complete analgesia or anaesthesia despite complete nerve interruption. Testing modalities can also pose challenges, since testing for thermal paw sensation involves heating up a large superficial and deep portion of the hindpaw that is innervated by both the sciatic and saphenous nerve. Finally, nerve injury is associated with the development of both peripheral and central features of neuropathic pain. In the setting of injury to only one sensory territory supplying the hindlimb, neuropathic pain can paradoxically heighten behavioural responses to sensory stimuli. Despite these caveats, by 28d post injury, when early hindpaw reinnervation had occurred, diabetic mice with PTEN knockdown were more sensitive to mechanical stimuli. No difference in thermal sensitivity was demonstrated.

Mechanisms that might account for regenerative failure in diabetic peripheral nerve have been widely considered. Reviewed elsewhere in detail [Kennedy and Zochodne2005b;Yasuda, Terada, Maeda, Kogawa, Sanada, Haneda, Kashiwagi, and Kikkawa2003], these have included abnormal polyol flux [Love *et al.* 1995;Yasuda, Terada, Taniguchi, Sasaki, Maeda, Haneda, Kashiwagi, and Kikkawa1999],

microangiopathy [Kennedy and Zochodne2002;Yamamoto *et al.* 1998], attenuated expression of neurotrophic receptors [Zochodne, Verge, Cheng, Sun, and Johnston2001], delayed upregulation of regeneration associated genes [Xu, Pierson, Murakawa, and Sima2002;Xu and Sima2001], failed IGF signaling [Glazner *et al.* 1993;Ishii and Lupien1995], 'effete' Schwann cells that fail to support axons, defective inflammatory clearance of the products of Wallerian degeneration [Conti *et al.* 1997;Terada, Yasuda, and Kikkawa1998] and abnormalities of structural axon proteins [Terada, Yasuda, and Kikkawa1998;Williams *et al.* 1982]. The linkage of impaired regeneration in diabetes to PTEN expression is novel and was unexpected. The mechanisms that upregulate PTEN are a matter of conjecture, not explored here, but of significant importance in understanding why diabetic axons regenerate less well. In muscle and endothelial cells, upregulation of PTEN associated with diabetes has been linked to palmitic acid acting through p38 MAPK and ATF-2 [Hu *et al.* 2007;Wang *et al.* 2006]. How PTEN might be influenced by mechanisms described above is uncertain. While it is likely that PTEN is expressed in lower levels in glial and other noneuronal cells, its major expression in this and previous work was neuronal, suggesting a direct interaction between diabetes and neuronal PTEN synthesis. In nondiabetic nerves, PTEN expression is downregulated after injury but residual expression nonetheless attenuated regenerative outgrowth [Christie, Webber, Martinez, Singh, and Zochodne2010]. In the setting of heightened expression, its importance may be correspondingly greater, a possibility suggested in our comparative studies of knockdown in littermate diabetic and nondiabetic mice. Similarly, upregulation of PTEN in small caliber IB-4 neurons has been linked to their limited growth capacity [Christie,

Webber, Martinez, Singh, and Zochodne2010;Leclere, Norman, Groutsi, Coffin, Mayer, Pizzey, and Tonge2007].

The mechanisms of siRNA retrograde transport to parent neurons, as demonstrated in this work, are unknown but may be similar to those involving viral vectors [Kaspar *et al.* 2002]. Recent findings also indicate that small RNA species may undergo significant intercellular exchange [Chitwood and Timmermans 2010]. That siRNA lends itself to axonal capture and selective retrograde uptake by injured neurons is of exceptional importance. The present work confirms similar observations in previous published [Webber, Christie, Cheng, Martinez, Singh, Singh, Thomas, and Zochodne2011a] and unpublished work from our laboratory using a variety of targeted siRNAs. Although the efficiency of transport and retrograde gene knockdown may be less than with viral vectors, this approach nonetheless offers a pathogen-free solution to targeted neuronal delivery. Since PTEN is a tumour suppressor molecule [Ali *et al.* 1999;Waite and Eng 2002], it is of translational interest to strictly circumscribe its potential role in both time and tissue. PTEN mutations are associated with Cowden syndrome, a disorder of cutaneous hamartomas with enhanced susceptibility to carcinoma, and with glioblastoma development [Mellinghoff *et al.* 2005]. To avoid potential oncogenesis, direct and selective neuronal delivery during critical periods of early axon outgrowth are required .

Taken together, our findings demonstrate that nonviral strategies for selective targeting of neurons may offer a new approach toward treating localized injuries. More importantly, we show that PTEN targeting offers interesting and significant benefits to diabetic regenerating axons, over and above the lesser impacts discovered in

nondiabetic axons. The importance of PTEN in understanding diabetic complications comes as a surprise, since a variety of intrinsic and extrinsic mechanisms of neuroregenerative failure have long been considered. Our results do not exclude these mechanisms, but may be superimposed, adding a novel but apparently detrimental response to diabetic nerve injury.

### **Acknowledgements**

Operating funds from Canadian Institutes of Health Research (CIHR) and the Canadian Diabetes Association (CDA) supported the work. BS holds a studentship from Alberta Innovates-Health Solutions (AI-HS). The authors do not have conflicts of interest with the material presented in this manuscript.

## Figures Legends

**Figure 1: PTEN expression is robustly elevated and extensive in adult diabetic sensory neurons.** A. PTEN mRNA transcripts in wild type (WT) and diabetic DRGs indicating higher expression of PTEN in diabetics. B. Western immunoblots labeled with PTEN in WT and diabetic DRGs before (basal, day 0) and 3 and 6d after sciatic nerve injury. Beta actin is used as a loading control. C. Quantification of protein data from B. Note: a robust rise in basal expression of PTEN protein in diabetic DRGs compared to nondiabetics. D. Examples of adult sensory neurons from WT, STZ induced type 1 diabetic, and db/db, type 2 diabetic DRGs labeled with PTEN (green). Note that PTEN is expressed in larger number of neurons with brighter luminosity in diabetics. E. Neuronal size analysis from WT and type 1 diabetic sensory neurons indicating a wider expression of PTEN. PTEN expression is significantly higher in smaller neurons with concurrent expression in large caliber sensory neurons in diabetics. F. Quantification of neuronal luminosity (described in methods section). Note a shift in percentage of neurons with higher luminosity intensity specifically in type 1 diabetes compared to controls. G. PTEN mRNA levels in WT and diabetic DRGs 3d after sciatic nerve injury H. WT and type 1 diabetic DRGs immunostained with PTEN (green), before (basal, day 0) and 3 and 6d after sciatic nerve injury. I, J: Marked decline in ps6k protein in adult 3 months diabetic DRGs and littermate controls analysed using western blot (I) and immunostaining (J). ps6k is prominently expressed in sensory neurons. For each of immunohistochemistry, western blotting and qRT-PCR experiment, n=3-5 animals per group/time point was used. [Values are mean  $\pm$  SEM; A,C,G,E, \* $p \leq 0.05$  Student's t-test

(one tailed in A,G,E (#), two tailed otherwise); F, \*  $p \leq 0.05$ , \*\*,  $p < 0.01$ , one way ANOVA; post hoc Tukey's multiple comparison test]. Scale bar = 50  $\mu\text{m}$ .

**Figure 2: PTEN inhibition increased neurite outgrowth of adult diabetic sensory neurons.** A. Fluorescent-labeled PTEN siRNA was integrated in to adult diabetic sensory neuron *in vitro*. The right panel represents a bright field image showing the neuronal cell body and neurites [Scale bar = 100  $\mu\text{m}$ ]. Also illustrated are high power views of single neurons. [Scale bar = 50  $\mu\text{m}$ ]. B. *in vitro*, PTEN mRNA transcripts in isolated sensory neurons with the siRNA ( $p = 0.07$  one tailed Student's t-test). C. Representative images of adult wild type and type 1 diabetic sensory neurons *in vitro* were labeled with an antibody to neurofilament (NF-200, red, [Scale bar = 100  $\mu\text{m}$ ]). Sensory neurons were exposed to culture media containing either scrambled or PTEN siRNA (20nM). D-G: Quantification of the total neurite outgrowth (D), mean number of branches per primary branch (E), mean number of processes per cell (processes extending from the soma) (F) and longest neurite (G). Note that PTEN siRNA increased outgrowth under both diabetic and non-diabetic conditions but its impact was greater in diabetic sensory neurons. Values are represented as mean  $\pm$  SEM [D-G, #  $p < 0.05$ , one tailed; \* $p < 0.05$ , two tailed Student's t-test].

**Figure 3: Local PTEN siRNA is retrogradely transported to alter gene expression in ipsilateral parent DRG sensory neurons** A. Administration of PTEN siRNA locally at the sciatic nerve and additional intraplantar injections successfully knocked down the PTEN mRNA expression in ipsilateral DRGs ( $n = 3$  separate experiments). B, C: Western immunoblot of DRG and sciatic lysates labeled with PTEN. Partial knockdown of PTEN protein in the ipsilateral DRGs (B) and locally in the sciatic nerve (C) ( $n = 3$

mice/treatment). D. Labeling of ipsilateral DRG sensory neurons with PTEN (green, [Scale bar =50  $\mu$ m]). PTEN luminosity decreased after siRNA application in ipsilateral DRGs similar to changes demonstrated with western immunoblots (B) and with qRT-PCR (A). E. Accumulation of fluorescent PTEN siRNA distal to the ligation site and proximal to the injury and siRNA delivery site indicating possible retrograde transport. The bright field and merged view are also shown. Values are represented as mean  $\pm$  SEM [A, \*  $p < 0.05$ , two tailed Student's t-test].

**Figure 4: Chronic diabetes is associated with electrophysiological and behavioural features of polyneuropathy.** A,B: Blood glucose levels 2 months after STZ injection were significantly higher (A) and gain in body weight was reduced in outbred diabetic mice compared to WT nondiabetic controls (B). C-E: Electrophysiological recordings of control and diabetic nerves. CMAP amplitudes and motor and sensory CVs were significantly reduced in 2 month old diabetics (C-E) with no change in SNAP amplitudes (F). G,H: diabetic animals were hyposensitive to mechanical (G) and thermal stimuli (H). A total of 10 WT and 26 type 1 diabetic animals were analysed. Values are represented as mean  $\pm$  SEM [A-H,\* $p < 0.05$ , \*\* $p < 0.01$ , \*\*\* $p < 0.001$ , two tailed Student's t-test].

**Figure 5: Knockdown of PTEN at the neuronal DRG cell body is associated with electrophysiological recovery in diabetics.** A,B: CMAPs in WT (A) and diabetics (B) before (day 0) and 14 and 28 days after injury (dpi). Preinjured CMAP amplitudes were lower in diabetics compared to littermate controls. CMAPs were reduced after sciatic nerve injury in both WT and diabetics (14dpi in A and B). PTEN inhibition was associated with significant improvement of CMAP amplitudes in both diabetics and

nondiabetics but amplitudes were almost double in diabetics compared to controls at day 28dpi (A,B). C,D: Motor CVs were lower in diabetics (D) than WT (C) before injury (day 0) and similarly at 14dpi. Recovery in motor CVs was significant only in diabetics exposed to PTEN siRNA (D). E,F: Sensory CVs in WT (E) and diabetics (F) before and 14 and 28dpi. Preinjured levels were lower in diabetics (day 0) (F) than control (E), and improved with the PTEN inhibition in both groups. G,H: SNAP amplitudes before and after injury in WT (G) and diabetics (H). A significant benefit on SNAP amplitudes using PTEN siRNA was noted only in nondiabetics but there was a similar trend in nondiabetics (G,H). Values are represented as mean  $\pm$  SEM [A-H, #,  $p < 0.05$ , one tailed Student's t-test; \* $p < 0.05$ , \*\* $p < 0.01$ , \*\*\* $p < 0.001$ , one way ANOVA; post hoc Tukey's multiple comparison test,  $n = 6-8$  animals/group/time point]. Scale bar = 100  $\mu\text{m}$ .

**Figure 6: Repopulation of myelinated axons and skin target reinnervation with PTEN knockdown.** A. Representative images of semithin sections of regenerating distal tibial nerve (10 mm from the injury site) from WT and diabetics 21 days after sciatic nerve injury with and without PTEN siRNA. B, C: Quantification of total myelinated axons (B) and axon caliber (C) measured as mean axonal diameter. Diabetic animals displayed regeneration deficits with significantly fewer and smaller caliber axons regenerating 3 weeks after injury. PTEN inhibition partially rescued the deficit. D. Representative images of footpads from WT and diabetics with and without PTEN siRNA indicating newly regenerating sensory afferents in the epidermis. Reinnervation was reduced in diabetics with very few reinnervating axons crossing into the epidermis. E,F: Quantification of vertical skin fiber density (E) and total skin fiber density (F) identifying lower numbers in diabetics. These deficits were rescued by PTEN

inhibition in diabetics but not in nondiabetics. Values are represented as mean  $\pm$  SEM [B,C, \* $p \leq 0.05$ , \*\* $p < 0.01$ , one way ANOVA; post hoc Tukey's multiple comparison tests and two-tailed Student's t-test, #one tailed Student's t-test, n=5-7 animals/group; E,F \* $p \leq 0.05$ , \*\* $p < 0.01$ , one way ANOVA; post hoc Tukey's multiple comparison test and two tailed Student's t-test; \* $p \leq 0.05$ ]. Scale bar; A=50  $\mu\text{m}$  and D=100  $\mu\text{m}$ .

For Peer Review

## References

- Ali IU, Schriml LM, Dean M. Mutational spectra of PTEN/MMAC1 gene: a tumor suppressor with lipid phosphatase activity  
12. J Natl Cancer Inst 1999; 91: 1922-1932.
- Andersen PL, Webber CA, Kimura KA, Schreyer DJ. Cyclic AMP prevents an increase in GAP-43 but promotes neurite growth in cultured adult rat dorsal root ganglion neurons. Exp Neurol 2000; 166: 153-165.
- Brewster WJ, Fernyhough P, Diemel LT, Mohiuddin L, Tomlinson DR. Diabetic neuropathy, nerve growth factor and other neurotrophic factors. Trends Neurosci 1994; 17: 321-325.
- Bril V. Role of electrophysiological studies in diabetic neuropathy. Can J Neurol Sci 1994; 21 Suppl: S8-S12.
- Carter AN, Downes CP. Phosphatidylinositol 3-kinase is activated by nerve growth factor and epidermal growth factor in PC12 cells. J Biol Chem 1992; 267: 14563-14567.
- Cheng C, Guo GF, Martinez JA, Singh V, Zochodne DW. Dynamic plasticity of axons within a cutaneous milieu. J Neurosci 2010; 30: 14735-14744.
- Chitwood DH, Timmermans MC. Small RNAs are on the move. Nature 2010; 467: 415-419.
- Christie KJ, Webber CA, Martinez JA, Singh B, Zochodne DW. PTEN inhibition to facilitate intrinsic regenerative outgrowth of adult peripheral axons. J Neurosci 2010; 30: 9306-9315.
- Conti G, Stoll G, Scarpini E *et al.* p75 neurotrophin receptor induction and macrophage infiltration in peripheral nerve during experimental diabetic neuropathy: possible relevance on regeneration. Exp Neurol 1997; 146: 206-211.
- Dyck PJ, Kratz KM, Karnes JL *et al.* The prevalence by staged severity of various types of diabetic neuropathy, retinopathy, and nephropathy in a population-based cohort: The Rochester Diabetic Neuropathy Study. Neurology 1993; 43: 817-824.
- Eickholt BJ, Walsh FS, Doherty P. An inactive pool of GSK-3 at the leading edge of growth cones is implicated in Semaphorin 3A signaling. J Cell Biol 2002; 157: 211-217.
- Gallo G, Letourneau PC. Localized sources of neurotrophins initiate axon collateral sprouting. J Neurosci 1998; 18: 5403-5414.
- Glazner GW, Lupien S, Miller JA, Ishii DN. Insulin-like growth factor II increases the rate of sciatic nerve regeneration in rats. Neuroscience 1993; 54: 791-797.

GrandPre T, Li S, Strittmatter SM. Nogo-66 receptor antagonist peptide promotes axonal regeneration. *Nature* 2002; 417: 547-551.

Hargreaves K, Dubner R, Brown F, Flores C, Joris J. A new and sensitive method for measuring thermal nociception in cutaneous hyperalgesia. *Pain* 1988; 32: 77-88.

Hu Z, Lee IH, Wang X *et al.* PTEN expression contributes to the regulation of muscle protein degradation in diabetes. *Diabetes* 2007; 56: 2449-2456.

Ishii DN, Lupien SB. Insulin-like growth factors protect against diabetic neuropathy: effects on sensory nerve regeneration in rats. *J Neurosci Res* 1995; 40: 138-144.

Jones DM, Tucker BA, Rahimtula M, Mearow KM. The synergistic effects of NGF and IGF-1 on neurite growth in adult sensory neurons: convergence on the PI 3-kinase signaling pathway. *J Neurochem* 2003; 86: 1116-1128.

Kan M, Guo G, Singh B, Singh V, Zochodne DW. Glucagon-like peptide 1, insulin, sensory neurons, and diabetic neuropathy. *J Neuropathol Exp Neurol* 2012; 71: 494-510.

Kaspar BK, Erickson D, Schaffer D, Hinh L, Gage FH, Peterson DA. Targeted retrograde gene delivery for neuronal protection. *Mol Ther* 2002; 5: 50-56.

Kennedy JM, Zochodne DW. The regenerative deficit of peripheral nerves in experimental diabetes: its extent, timing and possible mechanisms. *Brain* 2000; 123: 2118-2129.

Kennedy JM, Zochodne DW. Influence of experimental diabetes on the microcirculation of injured peripheral nerve. Functional and morphological aspects. *Diabetes* 2002; 51: 2233-2240.

Kennedy JM, Zochodne DW. Experimental diabetic neuropathy and spontaneous recovery: Is there irreparable damage? *Diabetes* 2005a; 54: 830-837.

Kennedy JM, Zochodne DW. Impaired peripheral nerve regeneration in diabetes mellitus. *J Peripher Nerv Syst* 2005b; 10: 144-157.

Kennedy WR, Navarro X, Goetz FC, Sutherland DE, Najarian JS. Effects of pancreatic transplantation on diabetic neuropathy. *N Engl J Med* 1990; 322: 1031-1037.

Leclere PG, Norman E, Groutsi F *et al.* Impaired axonal regeneration by isolectin B4-binding dorsal root ganglion neurons in vitro. *J Neurosci* 2007; 27: 1190-1199.

Leslie NR, Downes CP. PTEN: The down side of PI 3-kinase signalling. *Cell Signal* 2002; 14: 285-295.

Lindsay RM. Nerve growth factors (NGF, BDNF) enhance axonal regeneration but are not required for survival of adult sensory neurons. *J Neurosci* 1988; 8: 2394-2405.

Liu K, Lu Y, Lee JK *et al.* PTEN deletion enhances the regenerative ability of adult corticospinal neurons. *Nat Neurosci* 2010; 13: 1075-1081.

Longo FM, Powell HC, Lebeau J, Gerrero MR, Heckman H, Myers RR. Delayed nerve regeneration in streptozotocin diabetic rats. *Muscle Nerve* 1986; 9: 385-393.

Love A, Cotter MA, Cameron NE. Impaired myelinated fiber regeneration following freeze-injury in rats with streptozotocin-induced diabetes: involvement of the polyol pathway. *Brain Res* 1995; 703: 105-110.

Malik RA, Veves A, Walker D *et al.* Sural nerve fibre pathology in diabetic patients with mild neuropathy: relationship to pain, quantitative sensory testing and peripheral nerve electrophysiology. *Acta Neuropathol* 2001; 101: 367-374.

Mehra S, Tavakoli M, Kallinikos PA *et al.* Corneal confocal microscopy detects early nerve regeneration after pancreas transplantation in patients with type 1 diabetes. *Diabetes Care* 2007; 30: 2608-2612.

Mellinghoff IK, Wang MY, Vivanco I *et al.* Molecular determinants of the response of glioblastomas to EGFR kinase inhibitors. *N Engl J Med* 2005; 353: 2012-2024.

Mukhopadhyay G, Koherty P, Walsh FS, Crocker PR, Filbin MT. A novel role for myelin-associated glycoprotein as an inhibitor of axonal regeneration. *Neuron* 1994; 13: 757-767.

Ohnishi A, O'Brien PC, Dyck PJ. Studies to improve fixation of human nerves. Part 3. Effect of osmolality of glutaraldehyde solutions on relationship of axonal area to number of myelin lamellae. *J Neurol Sci* 1976; 27: 193-199.

Park KK, Liu K, Hu Y, Kanter JL, He Z. PTEN/mTOR and axon regeneration. *Exp Neurol* 2010; 223: 45-50.

Park KK, Liu K, Hu Y *et al.* Promoting axon regeneration in the adult CNS by modulation of the PTEN/mTOR pathway. *Science* 2008; 322: 963-966.

Polydefkis M, Hauer P, Griffin JW, McArthur JC. Skin biopsy as a tool to assess distal small fiber innervation in diabetic neuropathy. *Diabetes Technol Ther* 2001; 3: 23-28.

Raffioni S, Bradshaw RA. Activation of phosphatidylinositol 3-kinase by epidermal growth factor, basic fibroblast growth factor, and nerve growth factor in PC12 pheochromocytoma cells. *Proc Natl Acad Sci U S A* 1992; 89: 9121-9125.

Schnell L, Schneider R, Kolbeck R, Barde YA, Schwab ME. Neurotrophin-3 enhances sprouting of corticospinal tract during development and after adult spinal cord lesion. *Nature* 1994; 367: 170-173.

Sima AA, Bril V, Nathaniel V *et al.* Regeneration and repair of myelinated fibers in sural-nerve biopsy specimens from patients with diabetic neuropathy treated with sorbinil. *N Engl J Med* 1988; 319: 548-555.

Singh B, Xu Y, McLaughlin T *et al.* Resistance to trophic neurite outgrowth of sensory neurons exposed to insulin. *J Neurochem* 2012.

Soltoff SP, Rabin SL, Cantley LC, Kaplan DR. Nerve growth factor promotes the activation of phosphatidylinositol 3-kinase and its association with the trk tyrosine kinase. *J Biol Chem* 1992; 267: 17472-17477.

Terada M, Yasuda H, Kikkawa R. Delayed Wallerian degeneration and increased neurofilament phosphorylation in sciatic nerves of rats with streptozocin-induced diabetes. *J Neurol Sci* 1998; 155: 23-30.

Triban C, Guidolin D, Fabris M *et al.* Ganglioside treatment and improved axonal regeneration capacity in experimental diabetic neuropathy. *Diabetes* 1989; 38: 1012-1022.

Waite KA, Eng C. Protean PTEN: form and function. *Am J Hum Genet* 2002; 70: 829-844.

Wang XL, Zhang L, Youker K *et al.* Free fatty acids inhibit insulin signaling-stimulated endothelial nitric oxide synthase activation through upregulating PTEN or inhibiting Akt kinase. *Diabetes* 2006; 55: 2301-2310.

Webber CA, Christie KJ, Cheng C *et al.* Schwann cells direct peripheral nerve regeneration through the netrin-1 receptors, DCC and Unc5H2. *Glia* 2011; 59:1503-17.

Williams SK, Howarth NL, Devenny JJ, Bitensky MW. Structural and functional consequences of increased tubulin glycosylation in diabetes mellitus. *Proc Natl Acad Sci U S A* 1982; 79: 6546-6550.

Xu G, Pierson CR, Murakawa Y, Sima AA. Altered tubulin and neurofilament expression and impaired axonal growth in diabetic nerve regeneration. *J Neuropathol Exp Neurol* 2002; 61: 164-175.

Xu G, Sima AA. Altered immediate early gene expression in injured diabetic nerve: implications in regeneration. *J Neuropathol Exp Neurol* 2001; 60: 972-983.

Yamamoto Y, Yasuda Y, Kimura Y, Komiya Y. Effects of cilostazol, an antiplatelet agent, on axonal regeneration following nerve injury in diabetic rats. *Eur J Pharmacol* 1998; 352: 171-178.

Yasuda H, Terada M, Maeda K *et al.* Diabetic neuropathy and nerve regeneration. *Prog Neurobiol* 2003; 69: 229-285.

Yasuda H, Terada M, Taniguchi Y *et al*. Duplicate Use 15870 Impaired regeneration and no amelioration with aldose reductase inhibitor in crushed unmyelinated nerve fibers of diabetic rats. *NeuroReport* 1999; 10: 2405-2409.

Zherebitskaya E, Akude E, Smith DR, Fernyhough P. Development of selective axonopathy in adult sensory neurons isolated from diabetic rats: role of glucose-induced oxidative stress. *Diabetes* 2009; 58: 1356-1364.

Zochodne DW. Diabetic neuropathies: features and mechanisms. *Brain Pathol* 1999; 9: 369-391.

Zochodne DW, Ramji N, Toth C. Neuronal targeting in diabetes mellitus: a story of sensory neurons and motor neurons. *Neuroscientist* 2008; 14: 311-318.

Zochodne DW, Verge VMK, Cheng C, Sun H, Johnston J. Does diabetes target ganglion neurons? Progressive sensory neuron involvement in long term experimental diabetes. *Brain* 2001; 124: 2319-2334.

Peer Review

**Supplementary Figures:**

**Supplementary Figure 1:** PTEN expression was upregulated in diabetic sciatic nerve.

Western immunoblot of sciatic nerves harvested from STZ induced diabetics of 3 month and age matched littermate wild type controls were labeled with PTEN and actin (as control). Note that PTEN is expressed at higher levels in diabetic nerves.

**Supplementary Figure 2:** Rise in ps6k expression following PTEN inhibition. A.

Western immunoblot of ps6k in ipsilateral DRGs following PTEN inhibition. The ps6k band is overexpressed on the left (note actin bands) and matched for actin loading on the right. B. Immunostaining of ps6k in ipsilateral DRGs. Note that PTEN inhibition is associated with an apparent upregulation of ps6K in WT sensory neurons in ipsilateral DRGs. n=2-3 samples were used for western and immunoblots. Scale bar=100  $\mu$ m

**Supplementary Figure 3:** Behavioural changes associated with PTEN siRNA

treatment. A,B: Withdrawal response to noxious thermal stimuli in WT (A) and diabetics (B) using Hargreaves apparatus. Diabetics were hyposensitive to thermal stimuli at basal state (day 0, before injury). Fourteen days after injury, both diabetics and nondiabetics had trend towards hyposensitivity to thermal stimuli. PTEN inhibition had no significant impact on thermal sensation. C,D: Von Frey mechanical withdrawal test in WT (C) and diabetics (D). Withdrawal latency to a mechanical stimulus was higher in diabetics at baseline indicating hyposensitivity in these animals. At 14 and 28dpi diabetic treated with PTEN siRNA were more responsive. Values are represented as Mean  $\pm$  SEM [D #,  $p < 0.05$ , one tailed, \* $p < 0.05$ , two tailed Student's t-test. n=6-8 animals/group].

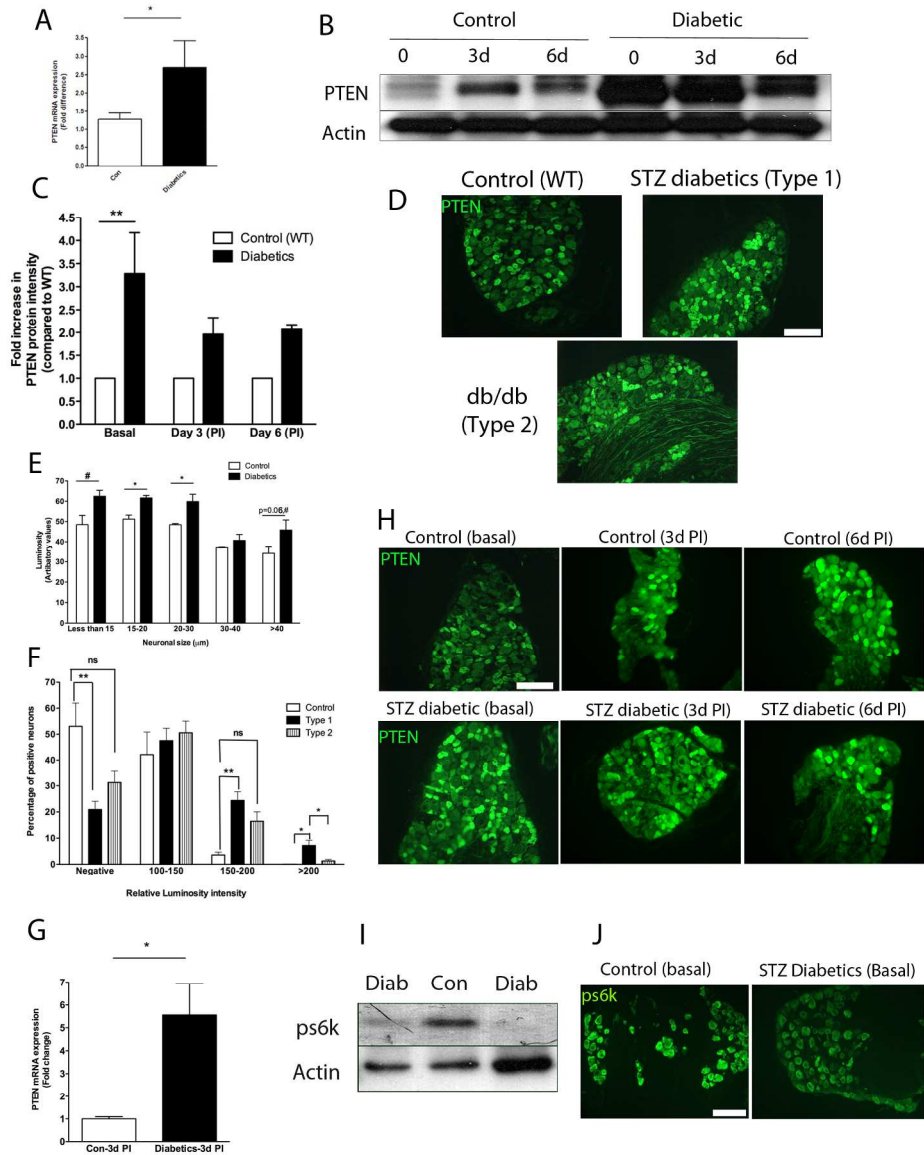


Figure 1  
203x254mm (300 x 300 DPI)

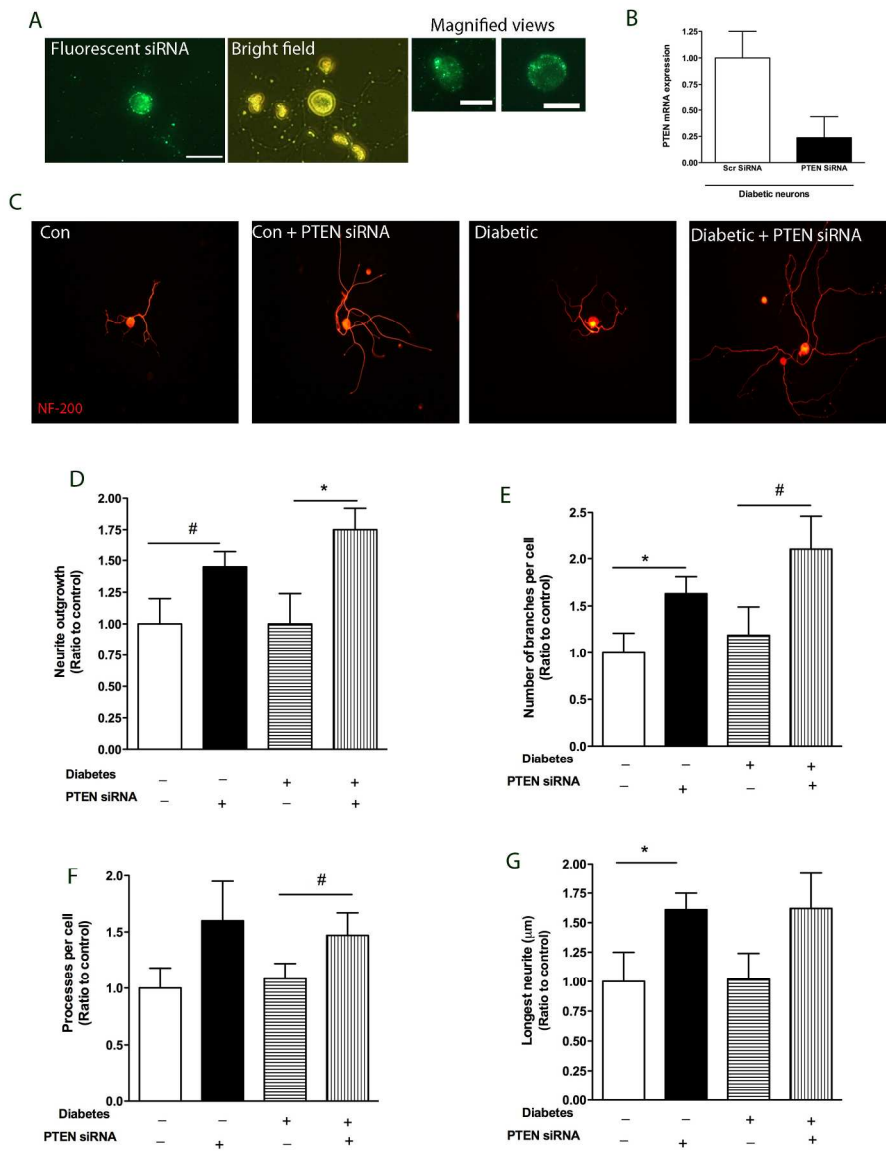


Figure 2  
203x254mm (300 x 300 DPI)

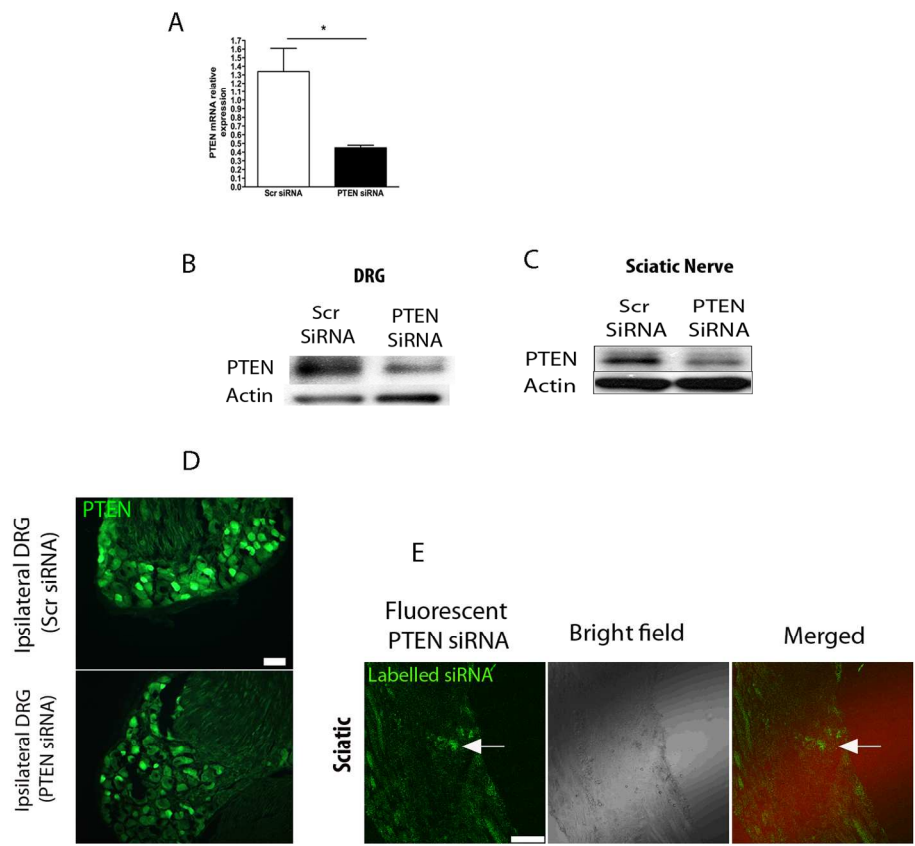
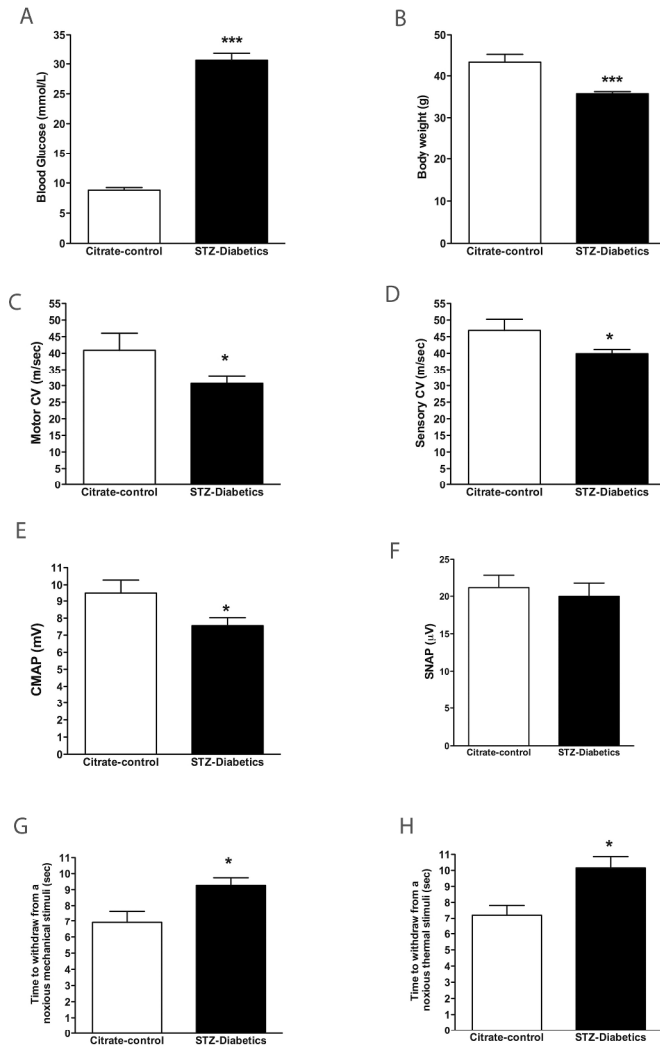


Figure 3  
203x254mm (300 x 300 DPI)



254x317mm (300 x 300 DPI)

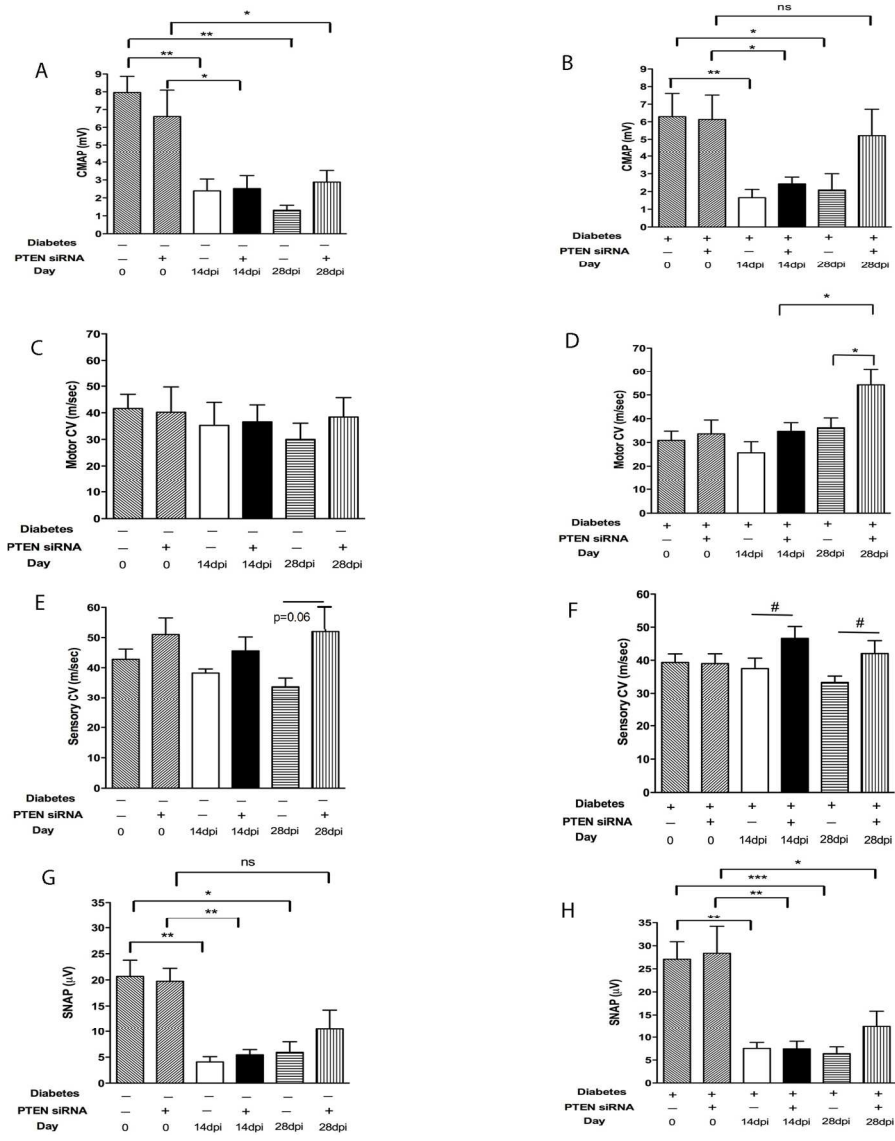


Figure 5  
203x259mm (300 x 300 DPI)

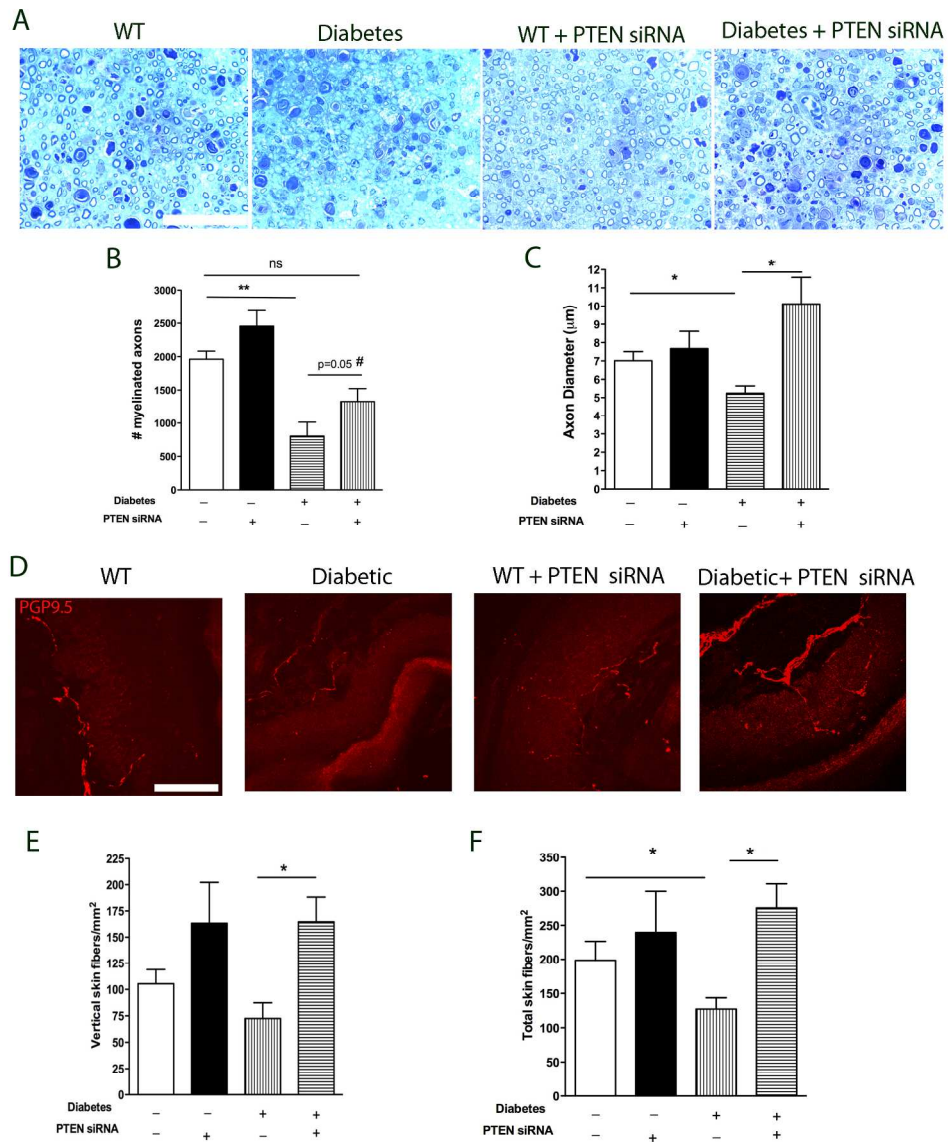
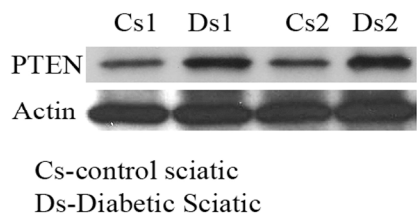
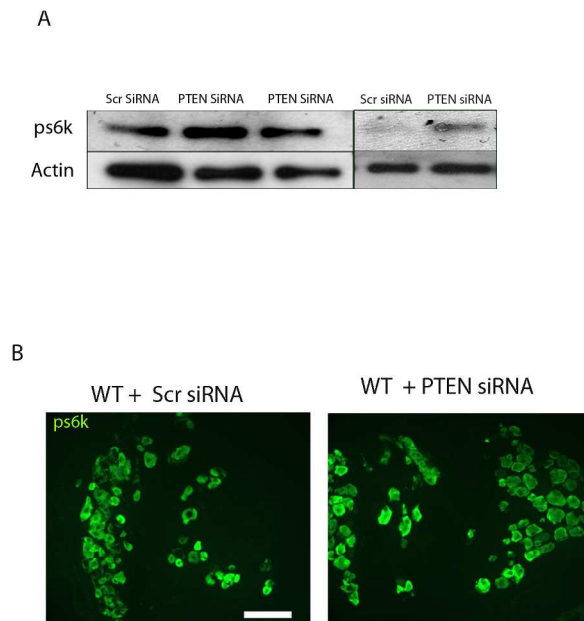


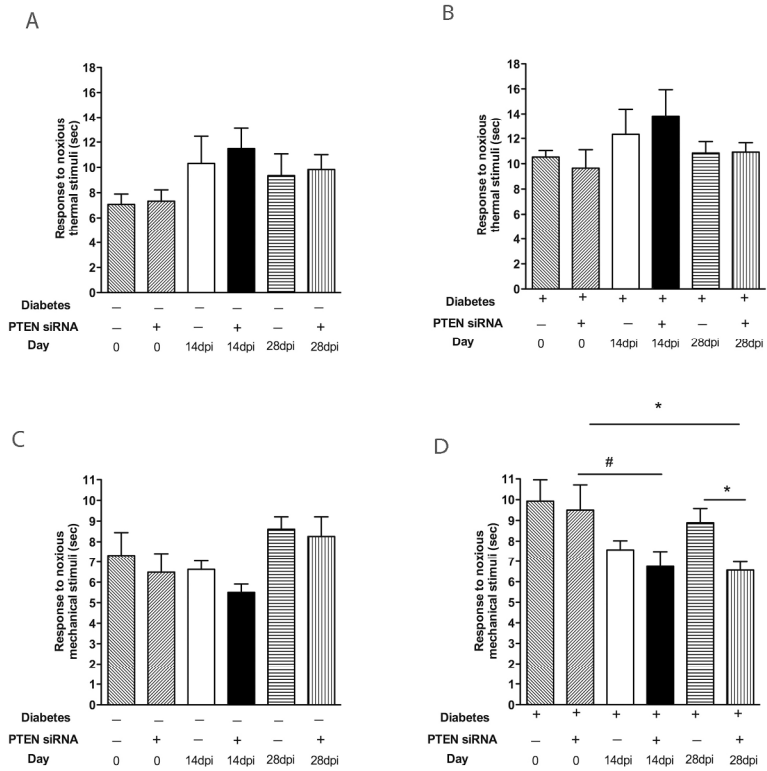
Figure 6  
203x254mm (300 x 300 DPI)



Supplementary Figure 1  
254x317mm (300 x 300 DPI)



Supplementary Figure 2  
203x254mm (300 x 300 DPI)



Supplementary Figure 3  
203x254mm (300 x 300 DPI)